RSC Advances

PAPER

View Article Online
View Journal | View Issue

Cite this: *RSC Adv.*, 2024, **14**, 15812

The synthesis and adsorption–dispersion properties of PPEGMA–PVPA copolymers in cement paste

Shenzhen Li, *[ab] Dongliang Zhou,[ab] Xin Shu,[ab] Qianping Ran*[abc] and Yong Yang[ab]

Received 9th March 2024
Accepted 2nd May 2024

DOI: 10.1039/d4ra01817f

rsc.li/rsc-advances

This study reports the synthesis of a novel superplasticizer, poly(poly(ethylene glycol)methacrylate)–poly(vinylphosphonic acid) (PPEGMA–PVPA), containing phosphate moieties *via* solution radical polymerization. By adjusting the feed ratios of monomers, PPEGMA–PVPA copolymers with different phosphate group densities were obtained, and their chemical structure was characterized *via* FT-IR, ^{1}H NMR spectroscopy and ICP-OES. The results demonstrated that about 70% of the VPA monomer was polymerized. The thermostability of PPEGMA–PVPA was also determined through DSC and TGA. The adsorption–dispersion performance onto cement pastes was investigated using mini-slump test, TOC and zeta potential analysis. It was demonstrated that the adsorption capacity of PPEGMA–PVPA onto cement paste was about 1.4 times stronger than that of the reference polycarboxylate superplasticizer and exhibited excellent adsorption–dispersion performance.

1 Introduction

Third generation superplasticizers generally have comb-shaped structures and consist of two necessary components: anionic anchor moieties and pendant moieties with steric hindrance.[1–4] During the last few decades, the structural improvement of the polycarboxylate superplasticizer has been mainly aimed at the sequence and molar proportion of these two polymer structural moieties,[5,6] and acrylic acid and methacrylic acid have been mainly utilized as polymerized precursors of carboxylate anchor moieties owing to their low cost and easy availability. However, with increasing research on the polycarboxylate superplasticizer, its performance improvement is slowly approaching the upper limit. In recent years, researchers have begun to look for other functional candidates as anchor moieties (*e.g.* the phosphate group[7–9] or silanol group[10–12]). Among these anchor candidates, the phosphate group with its strong complexing ability with calcium ions is considered the most efficient candidate to improve the adsorption–dispersion performance of superplasticizers. To date, several groups have reported the synthesis of copolymers containing phosphate groups and the performance characterization of the inorganic mineral phase.[8,13,14] Plank and coworkers[8] synthesized the copolymers of 2-hydroxyethyl methacrylate phosphate (HEMAP) and polyethylene glycol methacrylate ester and compared these phosphate polymers with polycarboxylate superplasticizers. Their results showed that the phosphate polymers have superior dispersing performance and exhibit comparable sulfate and clay tolerance as the conventional polycarboxylate superplasticizer. Ran and coworkers[14] reported that the polycarboxylate superplasticizers with phosphate groups exhibited excellent dispersion performance and relative low yield stress on account of their strong electrostatic effect and Ca^{2+} complexity. In these previous research studies, the same phosphate monomer HEMAP was selected. However, there are still some problems associated with the synthesis and preservation of HEMAP-containing copolymers that need to be resolved. For example, the poor water-solubility and unstable chemical structure of HEMAP make its ester bond prone to hydrolysis in alkaline cement pore solution.[15] In addition to HEMAP, vinylphosphonic acid (VPA) is another commercially available phosphate monomer.[16–18] The vinyl moiety of VPA is directly bonded to the phosphonic acid group. Therefore, the chemical structure of VPA is more compact than that of HEMAP.[19] Poly(vinylphosphonic acid) (PVPA) has displayed a high charge density under alkaline conditions owing to the high fraction of acid groups in the polymer chain, and VPA is considered a promising candidate for cement superplasticizers. Moreover, the good chemical stability and great water-solubility of VPA would predictably prevent some inconveniences in synthetic operation.

In recent years, increasing research studies on the polymerization and mechanism of VPA have been carried out. For example, Destarac and coworkers[20] reported the first RAFT/MADIX polymerization of VPA and the deblock co-oligomerization of AA (acrylic acid) and VPA using *O*-ethyl xanthate transfer agent in water. Tan and coworkers[21] investigated the copolymerization of VPA and acrylamide (AM), and tested the ability of copolymer

[a]*State Key Laboratory of High Performance Civil Engineering Materials, Nanjing 210008, China. E-mail: lishenzhen@cnjsjk.cn*

[b]*Sobute New Materials Co., Ltd, Nanjing 210008, China*

[c]*School of Materials Science and Engineering, Southeast University, Nanjing, 211189, China*

hydrogels to support cell adhesion and growth. Kabiri and coworkers[22] synthesized phosphonic acid-containing alcohol absorbents *via* solution polymerization using poly(ethylene glycol methyl ether methacrylate) (PEGMEMA), VPA and poly(ethylene glycol dimethacrylate) macro-crosslinker, and they found that the alcohol absorbency of these absorbents was proportional to the VPA proportion. Marty and coworkers[18] synthesized the poly(-ethylene glycol)–poly(vinyl phosphonic acid) block copolymers (PEG-*b*-PVPA) by RAFT/MADIX polymerization, and evaluated the structure–performance relationship of these polymer on stabilizing iron oxide nanoparticles. Budd and coworkers[19] reported the polymerization of AA and VPA, and investigated the calcium chelation affinity of these copolymers, which exhibited a maximum with a VPA content of *ca.* 30 mol%. Because of the outstanding characteristics, VPA has the potential to become a widely-used and high-performing functional monomer. Despite some progress in the above-mentioned cases, research studies on the polymerization and application of VPA is still faced with challenges, such as the improvement of the VPA conversion. As every coin has two sides, it is precisely because of these challenges that the synthesis of VPA-containing copolymers and the study of their properties are of great significance, especially in promoting the application in cement superplasticizers. Based on these previous researches, a phosphate-containing copolymer was synthesized by solution radical copolymerization using VPA and poly(ethylene glycol)methacrylate (PEGMA) as monomers, and characterized by Fourier-transform infrared spectroscopy (FT-IR) and ^{1}H nuclear magnetic resonance spectroscopy (^{1}H NMR) spectra. Subsequently, the molar ratios of two monomer units were calculated according to the ^{1}H NMR and inductively coupled plasma-optical emission spectroscopy (ICP-OES) data, and then the thermal stability of the synthesized polymers was investigated by thermogravimetric analysis (TGA) and differential scanning calorimetry (DSC) analysis. Finally, the adsorption–dispersion capacity of the synthesized polymers onto cement pastes was investigated by means of mini-slump test, total organic carbon (TOC) and zeta potential analysis.

2 Materials and methods

2.1 Raw material

Vinylphosphonic acid (VPA, 95%, stabilized with 5–7% H_2O, Bidepharm, China) and methacrylic acid (MAA, 99%, stabilized with 250 ppm MEHQ, Innochem, China) were used as received without further purification. 2,2′-Azobis(2-methylpropionitrile) (AIBN, 98%, Innochem, China) was recrystallized from ethanol and stored at −20 °C before use. 2,2′-Azobis(2-methylpropionamidine)dihydrochloride (AIBA, 97%, Sigma-aldrich, USA) was used without further purification. 2-Mercaptoethanol (BME) was used as a chain transfer agent without further purification. Poly(ethylene glycol)methyl ether methacrylate (PEGMA, $M_w = 1000$ g mol^{-1}) was synthesized as reported previously.[23] Deionized water, ethyl acetate (EtOAc, 99+%, Innochem, China), dichloromethane (DCM, 99+%, Innochem, China) were also used.

Ordinary Portland cement (cement P.II 52.5, Jiangnan-Onoda Cement Co., Ltd), according to the Chinese standard GB 175-2007 (NSPRC, 2007), was used in this work. The specific surface area determined by the Blaine method was 352 m^2 kg^{-1}. Its chemical composition was determined using X-ray fluorescence spectrometry (ARL Advant'XP, Thermo Fisher, USA) and shown in Table 1, and it phase composition was quantified by X-ray diffraction (D8 Discover, Bruker-AXS, Germany) and detailed in Table 2.

2.2 Sample preparation and test methods

2.2.1 Synthesis of poly(poly(ethylene glycol)methacrylate)–poly(vinylphosphonic acid) (PPEGMA–PVPA). Four comb polymers of PPEGMA–PVPA were synthesized *via* free radical copolymerization of VPA and PEGMA and denominated as PV4A, PV3A, PV2A and PV1A, which correspond to the molar ratios of 4 : 1, 3 : 1, 2 : 1 and 1 : 1, respectively. Here, a typical free radical polymerization of PV4A under the condition of $[VPA]_0$: $[PEGMA]_0 = 4:1$ with the monomer concentration of 30 wt% was introduced, and the other copolymers followed a similar procedure. Typically, VPA (5.0 g, 46.30 mmol), EtOAc (15.0 g) were added into a 100 mL Schlenk flask with a magnetic bar. The mixture solution was purged with nitrogen for 10 min and heated in a water bath at 70 °C for 0.5 h. The solution of PEGMA (1000 g mol^{-1}, 11.6 g, 11.60 mmol), AIBN (3 mol%, 230 mg, 1.39 mmol) and EtOAc (23.0 g) was added dropwise for the duration of 0.5 h under a nitrogen atmosphere, and then the reaction was maintained for 4 h at 70 °C. For the determination of the monomer conversion by ^{1}H NMR or GPC analysis, a polymer sample was obtained using a syringe with long needle at a certain time interval. After the polymerization was completed,

Table 1 Chemical composition and phase composition of the used cement

Chemical composition	Content (wt%)	Phase composition	Content (wt%)
Calcium oxide (CaO)	62.88	Tricalcium silicate (C_3S)	59.39
Silicon dioxide (SiO_2)	19.57	Dicalcium silicate (C_2S)	13.38
Aluminium oxide (Al_2O_3)	4.69	Tricalcium aluminate (C_3A)	9.08
Sulfur trioxide (SO_3)	3.69	Tetracalcium aluminoferrite (C_4AF)	7.61
Ferric oxide (Fe_2O_3)	3.04	Gypsum ($CaSO_4 \cdot 2H_2O$)	0.73
Magnesium oxide (MgO)	1.64	Bassanite ($CaSO_4 \cdot 1/2H_2O$)	2.07
Potassium oxide (K_2O)	0.56	Calcium sulfate ($CaSO_4$)	3.41
Sodium oxide (Na_2O)	0.17	Calcium carbonate ($CaCO_3$)	3.22
Total	96.24	Calcium hydroxide ($Ca(OH)_2$)	0.91
Loss on ignition	2.34	Silicon dioxide	0.22

Table 2 Monomer feed ratios and GPC results of the synthesized copolymers

Polymer sample	Molar ratio VPA : MAA : PEGMA	Conv. (%)	M_w (kg mol^{-1})	M_n (kg mol^{-1})	PDI
PV4A	4 : 0 : 1	80	10 700	7360	1.45
PV3A	3 : 0 : 1	71	10 500	6960	1.51
PV2A	2 : 0 : 1	77	11 100	7530	1.47
PV1A	1 : 0 : 1	78	14 800	9070	1.63
PVPA–PMAA	2 : 1 : 0	87	13 400	7370	1.81
PPEGMA–PAA	0 : 3 : 1	89	12 100	7880	1.53

the solvent EtOAc was removed using a rotary evaporator and then the sticky pale-yellow polymer was further purified using a dialysis membrane (cut-off range M_w = 3500 g mol^{-1}, Shanghai Yuanye Bio-Technology Co., Ltd, China). In addition, the elemental analysis was performed by atomic absorption spectroscopy (ICP-OES, optima 4300DV, PerkinElmer Inc.) to determine the proportion of VPA in the copolymers.

2.2.2 Synthesis of poly(vinylphosphonic acid)–poly(methacrylic acid) (PVPA–PMAA). PVPA–PMAA was synthesized by *via* free radical copolymerization of VPA and PMAA in EtOAc, and the specific reaction procedure was like that of PPEGMA–PVPA. VPA (2.5 g, 23.14 mmol) was accurately taken, dissolved, and diluted with anhydrous EtOAc (5.0 g). The colorless solution was purged with nitrogen for 10 min to deoxygenate the sample, and then heated at 70 °C for 0.5 h. The solution of MAA (3.98 g, 46.28 mmol), AIBN (4 mol%, 152 mg, 0.93 mmol), BME (0.5 mol%, 9 mg, 0.12 mol) and EtOAc (5.0 g) was added dropwise for 0.5 h under nitrogen atmosphere, and then the reaction was maintained for 4 h at 70 °C. After removing the solvent on a rotary evaporator, the obtained solid was dissolved in 7 mL DCM, followed by precipitation into cold diethyl ether, filtered and dried under vacuum overnight, and PVPA–PMAA ($M_{n,GPC}$ = 6.7 kg mol^{-1}, $M_{w,GPC}$ = 12.0 kg mol^{-1}, $Đ$ = 1.79) was obtained as a white powder.

2.2.3 Synthesis of PVPA. PVPA was synthesized by following the protocol of Wegner and coworkers with slight modification.[24] A solution of VPA (5.0 g, 46.28 mmol), AIBA (2 mol%, 250 mg, 0.93 mmol) and deionized water (2.0 g) were added to a Schlenk flask with a magnetic bar. The solution was purged with nitrogen for 10 min and then heated to 80 °C for two hours. The product was purified using a cellulose dialysis membrane (cut-off range M_w = 1000 g mol^{-1}, Shanghai Yuanye Bio-Technology Co., Ltd, China). The resulting polymer solution was removed using a rotary evaporator and then dried to a constant weight in a vacuum oven. $M_{n,GPC}$ = 5.6 kg mol^{-1}, $M_{w,GPC}$ = 7.9 kg mol^{-1}, $Đ$ = 1.41.

2.2.4 Structural characterization. ^{1}H NMR spectra of the synthesized polymers were determined on a Bruker Avance III 400 MHz NMR spectrometer with D_2O as solvent, and the FTIR spectra were recorded on a Bruker Tensor-27 FT-IR spectrometer under strictly constant conditions in the region of 400 to 4000 cm^{-1}. The monomer conversions of VPA and PEGMA were calculated by simple mathematical expressions using relative peak integrations of the ^{1}H NMR spectra. The molecular weight and the polydispersity index ($Đ = M_w/M_n$) of the polymers were characterized by gel permeation chromatography (GPC) equipped with a Waters 2695 GPC with two Waters Ultrahydrogel 250 columns (7.8 mm × 300 mm) and Waters 2414 refractive index detector using $NaNO_3$ aqueous solution (0.1 mol L^{-1}, pH = 12) as the eluent and relative to the polyethylene glycol standards. The phosphorus contents in the synthesized polymers were detected by inductively coupled plasma-optical emission spectroscopy (ICP-OES, Spectro Blue Sop, German), with the incident frequency of 27 MHZ and power of 1400 W.

2.2.5 Performance measurements

2.2.5.1 Mini-slump test. Fluidities and fluidity retentions of fresh cement paste containing the synthesized polymers was characterized by spread diameter through a mini-slump test based on the "GB/T 8077-2012" standard. The water/cement (w/c) ratio of the cement paste without polymers was 0.29, and then the dosage of synthesized polymers was 0.15% by cement weight. The synthesized polymers were dissolved in the required amount of mixing water prior to cement addition. 300 g of cement was added to the mixing water containing copolymers and slowly agitated for 2 min; the mixture was allowed to rest for 15 s without stirring and then rapidly stirred for another 2 min. The cement paste was immediately cast into a mini-slump cone (top diameter: 36 mm, bottom diameter: 60 mm and height: 60 mm) placed on a glass plate, and then the cone was vertically lifted. After waiting for 30 s, the resulting spread of the paste was measured twice, the second measurement being in a 90° angle to the first, and the average was taken to give the final spread value. For the fluidity-retention behavior of the paste, after each measurement, the cement paste was transferred back into the cup and covered with a wet towel in order to avoid drying. Before each subsequent measurement, the paste was stirred again for 1 min. Measurements were taken every 15 min over a total period of 60 min.

2.2.5.2 TOC analysis. The adsorption of the synthesized polymers on the cement paste was tested by total organic carbon apparatus (Multi N/C 3100, Analytik Jena AG, Germany). Generally, 100 g cement, 200 g deionized water containing certain amounts of polymers were mixed and stirred for 30 min, and then the mixture was separated by centrifuging at 10 000 rpm for 2 min to obtain the supernatant. After being diluted 10 times with deionized water, the total organic carbon of the supernatant was determined by combustion at 1000 °C. Measurements were generally repeated three times. The average adsorption amount of the polymers was calculated based on the reduction of the TOC content of samples before and after mixing with cement paste.

2.2.5.3 Zeta potential test. The zeta potential of cement pastes was determined using a zeta potential analyzer (DT-300, Dispersion Technology, USA). 10 g cement was added to 200 g deionized water containing various amounts of the synthesized polymers (0.1–0.25% bwoc) and stirred for 30 min, and then the mixture was separated by centrifuging at 10 000 rpm for 2 min to obtain the supernatant, which was used to record the zeta potential of the fresh cement pastes.

3 Results and discussion

3.1 The synthesis of PPEGMA–PVPA and structural characterization

Recently, several research groups have studied the synthetic methodology and polymeric kinetics of VPA and its derivatives. Different polymerization methods have been developed, such as free radical polymerization,[24] RAFT polymerization,[20,25] metal-catalytic polymerization[26] and others. In terms of the polymerization mechanism of VPA, Wegner and coworkers[24] reported that the radical polymerization of VPA proceeded *via* cyclopolymerization of the vinylphosphonic acid anhydride as an intermediate. Kabiri and coworkers[22] compared the polymerization of VPA in the aqueous and organic phase. They found that the production of an anhydride intermediate of VPA can be effectively promoted in ester solvents and thus VPA exhibited a higher polymerization activity. Based on these previous research studies, ethyl acetate (EtOAc) was used as the polymerization solvent in this work to prepare the superplasticizer containing the phosphate anchor group. The polymerization mechanism of VPA in EtOAc is shown in Fig. 1. Indeed, aqueous copolymerization is expected as the ideal synthetic system for the cement superplasticizer. However, even after our dedicated attempts at improving the reaction conditions, the aqueous copolymerization of VPA was still not satisfactory.

Here, the macromonomer PEGMA was chosen to introduce PEG graft chains for the preparation of the comb-type superplasticizer and a series of poly(vinylphosphonic acid)-*co*-poly(-poly(ethylene glycol)methyl ether methacrylate) (PPEGMA–PVPA) with different proportions of monomer units were synthesized. To clearly characterize the chemical structures of the VPA-containing copolymers, poly(vinyl phosphonic acid) (PVPA) and poly(vinyl phosphonic acid)-*co*-poly(methacrylic acid) (PVPA–PMAA) were synthesized as reference samples. The synthetic routes of these polymers are shown in Fig. 2. As a result, the proportion of monomer units in the copolymers could be determined by comparing the integral of the characteristic peak area of the ^{1}H NMR spectra. Otherwise, poly(-poly(ethylene glycol)methyl ether methacrylate)–poly(acrylic acid) (PPEGMA–PAA) was also synthesized following a method reported to evaluate the difference in the adsorption or dispersion activity between phosphate groups and carboxylic groups as the anionic anchor.[27] Table 2 exhibits the feed ratios of the monomers and the molecular properties of the synthesized polymer samples, displaying the weight-averaged molecular weights (M_w) and number-averaged molecular weights (M_n) and the polydispersity index (PDI). The monomer conversion was determined by comparing the integration of the GPC peak area in Fig. 3.

To verify the successful synthesis of PPEGMA–PVPA, the prepared polymers, PPEGMA–PVPA (including PV4A, PV3A, PV2A and PV1A) as well as PVPA–PMAA and PPEGMA–PAA, were further dialyzed against deionized water to remove the residual monomers, and the GPC traces before/after dialysis are shown in Fig. 3.

Then, the chemical structures of the purified copolymers were characterized using FT-IR and ^{1}H NMR spectra. As shown in Fig. 4a, the FT-IR spectra of all these polymers exhibited a set of medium-intensity absorption bands at 3600–2300 cm^{-1}. This is due to the methylene C–H stretching mode and the O–H stretching mode, and a strong band at 1690 cm^{-1} was attributed to the P–OH bend. The C=O stretch of the carboxyl groups of PVPA–PMAA or the ester groups of PV4A appears at 1710 cm^{-1}. The spectra of PVPA and PV4A exhibited a band at 950 cm^{-1}, representing the P=O stretch. The absorption bands of PV4A at 2900 cm^{-1} was related to the stretching vibration of the aliphatic C–H bonds of the PEG moieties. In addition, the ^{1}H NMR spectrum in D_2O was studied in detail to further clarify the chemical structure of the synthesized polymers and quantify the proportion of two monomer units in PV4A. The multi-

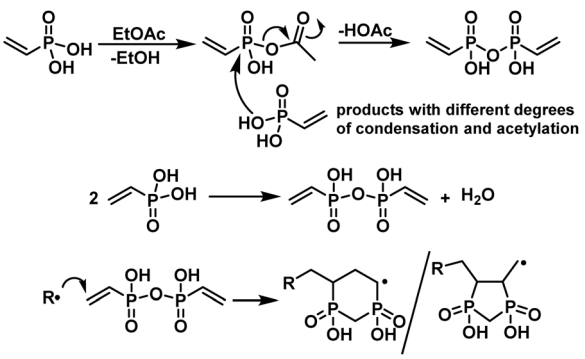

Fig. 1 The polymerization mechanism of VPA in EtOAc *via* vinylphosphonic acid anhydride.

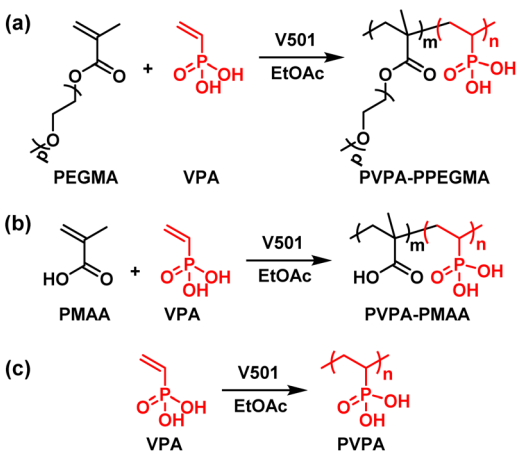

Fig. 2 The synthetic routes of PPEGMA–PVPA (a), PVPA–PMAA (b) and PVPA (c).

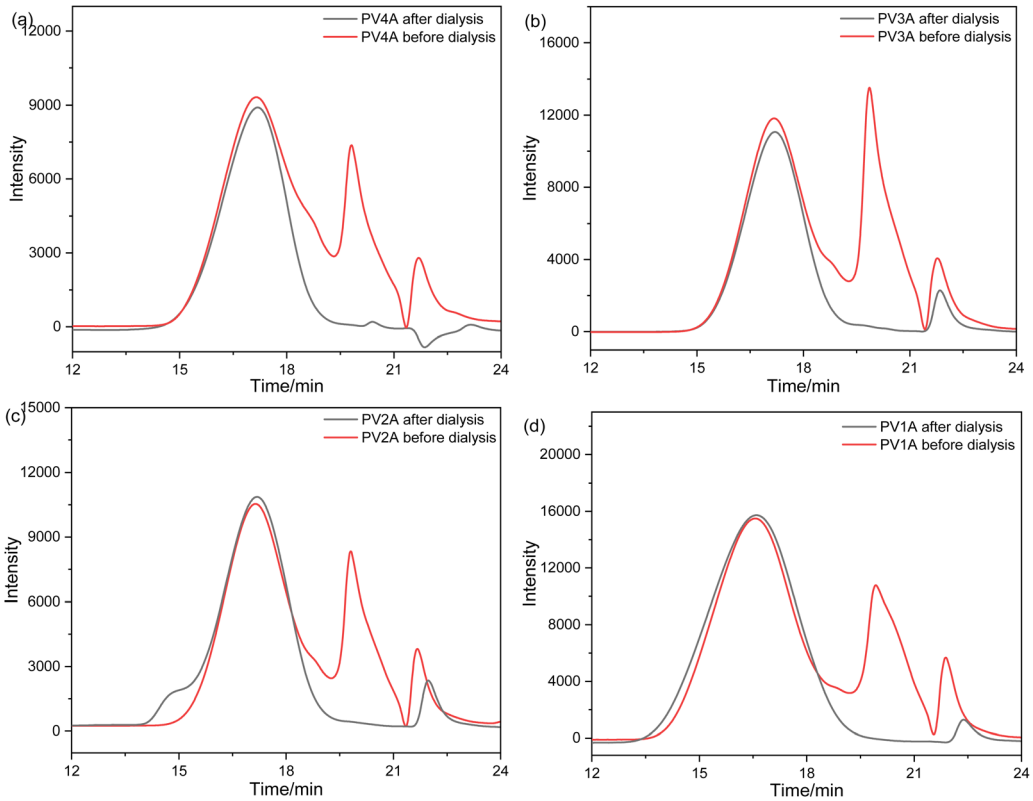

Fig. 3 GPC traces of the synthesized PV4A (a), PV3A (b), PV2A (c), PV1A (d) before/after dialysis.

resonances at the chemical shift ranges of 1.5–2.5 ppm (denoted as CH_2) were observed in all spectra and attributed to methylene protons of the VPA units,[28] while the spectra of PVPA–PMAA and PV4A exhibited the signal of methyl protons and methylene protons of MAA units at chemical shift ranges of 0.6–1.5 ppm (denoted as CH_3).[24] The ethylene oxide groups of the PEG moieties of PV4A appear at 3.5 ppm (denoted as OCH_2),[29] and the terminal methyl protons of the PEG moieties of PV4A appear at 3.2 ppm (denoted as OCH_3). It should be noted that the peaks at 1.00, 1.91 and 3.48 ppm in Fig. 5a were the signal peaks of the solvent ethyl acetate. All of the FT-IR and ^{1}H NMR results demonstrated the successful synthesis of PV4A.

Furthermore, two monomer unit ratios of PV4A can be determined by comparing the integral areas of the monomer protons. The function is described in eqn (1), and the calculation results showed that the molar ratio of VPA to PEGMA structural units in PV4A was about 3.3 : 1.

$$\text{mol\% VPA} = \frac{5I_{CH_2}}{5I_{CH_2} + 3I_{CH_3}} \times 100\% \quad (1)$$

In addition, the ^{1}H NMR spectra of the copolymerization of VPA and PEGMA over time were also obtained to monitor the reaction process. The monomer conversion can be obtained by calculating the integral area of characteristic peaks. As shown in

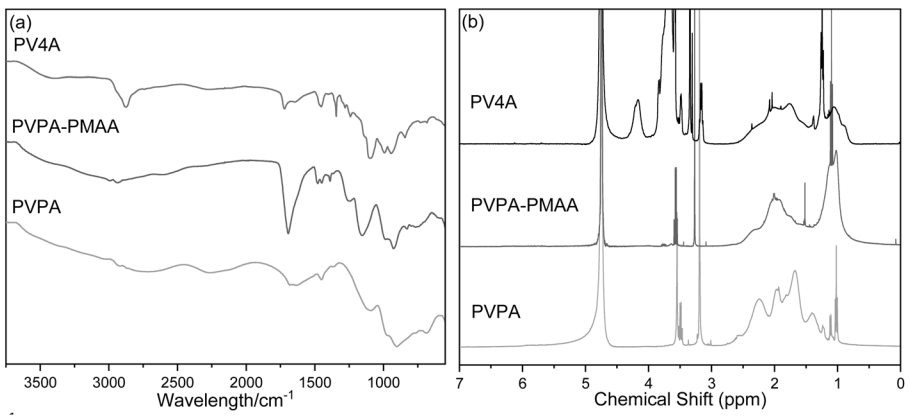

Fig. 4 The FT-IR (a) and ^{1}H NMR spectra (b) of PPEGMA–PVPA, PVPA–PMAA and PVPA.

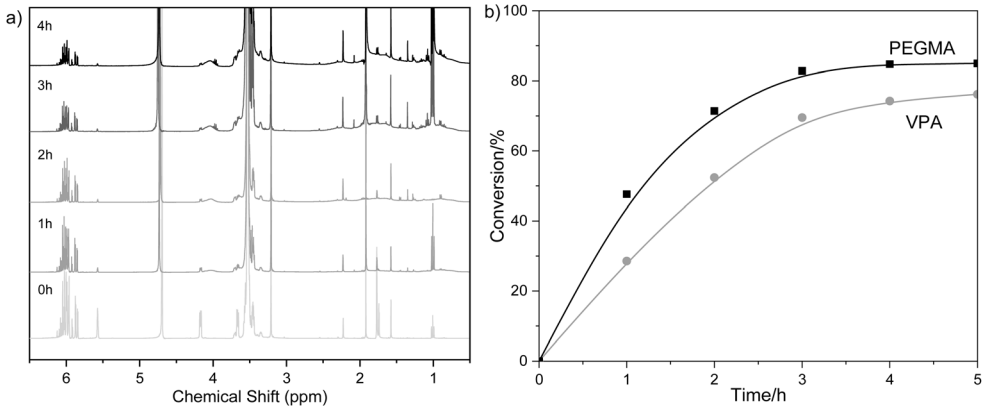

Fig. 5 (a) ^{1}H NMR spectra of the PV4A copolymerization in D_2O at different polymerization times, and (b) kinetic curves of the copolymerization of VPA and the PEGMA monomer.

Fig. 5a, the signal intensity of VPA vinyl-bond at 5.9–6.1 ppm gradually decreased over time, while the signal intensity of the methylene protons of the polymer backbone at 1.5–2.5 ppm increased. The sharp peak at 4.2 ppm, representing the methylene protons of the ester-bond of PEGMA moieties, gradually decreased, and a new wide peak appeared at 4.1 ppm, which was identified as the methylene protons of polymeric ester-bond. At the same time, the peaks of the copolymer backbone at 0.6–1.5 ppm increased. According to the ratios of the two residual monomers and the proportion of the structural units in the polymers at different times, the correlation between the monomer conversion and reaction time was obtained as shown in Fig. 5b. An attempt to evaluate the monomer conversion using the GPC curves failed. This was due to the strong overlap of monomer signals of VPA and PEGMA (Fig. 6). Nevertheless, by counting the overall conversion of the two monomers, the GPC curves can still be a useful means to detect the polymerization process.

Furthermore, inductively coupled plasma-optical emission spectroscopy (ICP-OES) was employed to measure the phosphorus content in these dialyzed polymers, and then the actual monomer proportions of PPEGMA–PVPA could be calculated by following eqn (2)–(4), in which w[VPA] designed refers to the designed mass percentage of VPA units, feed ratio refers to the molar ratio of VPA to PEGMA, c[P] refers to the concentration of phosphorous element in the tested polymer solution, c[polymer] refers to the measured concentration of the polymer solution, M[VPA] and M[P] refer to the molar mass of VPA and phosphorus element, respectively, and actual ratio refers to the proportion of two structural units in the synthesized polymer. As shown in Table 3, the actual weight percentage of the VPA monomer in PPEGMA–PVPA, obtained from ICP-OES analysis, was 30.1 wt% for PV4A, 24.5 wt% for PV3A, 17.8 wt% for PV2A and 9.7 wt% for PV1A. As a result, the experimental phosphorous content of PPEGMA–PVPA was lower than the designed value, and about 60% of the feed VPA monomer was reacted in copolymerization condition. The molar ratio of the monomer units of PV4A *via* ICP-OES was close to that obtained *via* ^{1}H NMR.

$$w[\mathrm{VPA}]_{\mathrm{designed}} = \frac{\text{feeding ratio} \times M[\mathrm{VPA}]}{\text{feeding ratio} \times M[\mathrm{VPA}] + M[\mathrm{PEGMA}]} \quad (2)$$

$$w[\mathrm{VPA}]_{\mathrm{actual}} = \frac{c[\mathrm{P}]}{c[\mathrm{polymer}]} \times \frac{M[\mathrm{VPA}]}{M[\mathrm{P}]} \quad (3)$$

$$\text{Actual ratio} = \frac{w[\mathrm{VPA}]_{\mathrm{actual}}}{w[\mathrm{VPA}]_{\mathrm{designed}}} \times \text{feeding ratio} \quad (4)$$

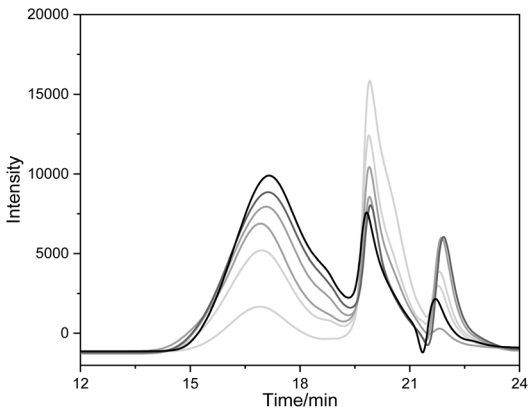

Fig. 6 GPC curves of the copolymerization between VPA and PEGMA at different polymerization times.

To rule out the presence of homogeneous PVPA polymers in these dialyzed polymers, DSC and TGA were employed to characterize the polymers by recording the phase and mass changes as a function of temperature (Fig. 7). A single endothermic peak at 37 °C was detected in the DSC thermogram of PV4A, and no significant peaks can be found in the temperature range of 90–130 °C where a glass transition temperature of PVPA was reported.[22] A TGA investigation was also carried out for PV4A from ambient temperature to 800 °C (Fig. 7). A three-stage decomposition and a 18% char yield were observed due to the phosphate groups in the PV4A structure. These results further illustrate the successful synthesis of PPEGMA–PVPA polymers.

Table 3 The ICP-OES results and the actual monomer ratios of the synthesized PPEGMA–PVPA[a]

Polymer sample	Feed ratio VPA : PEGMA	w[P][b] (wt%)	$w[VPA]_{actual}$[c] (wt%)	$w[VPA]_{designed}$[d] (wt%)	Actual ratio VPA : PEGMA
PV4A	4 : 1	6.7	23.3	30.1	3.1 : 1
PV3A	3 : 1	4.9	17.1	24.5	2.1 : 1
PV2A	2 : 1	3.2	11.1	17.8	1.3 : 1
PV1A	1 : 1	1.7	5.8	9.7	0.6 : 1

[a] Polymer concentration was 500 mg L^{-1}. [b] Phosphorous content of PPEGMA–PVPA determined by ICP-OES. [c] Actual VPA content of PPEGMA–PVPA calculated by eqn (3). [d] Designed VPA content of PPEGMA–PVPA.

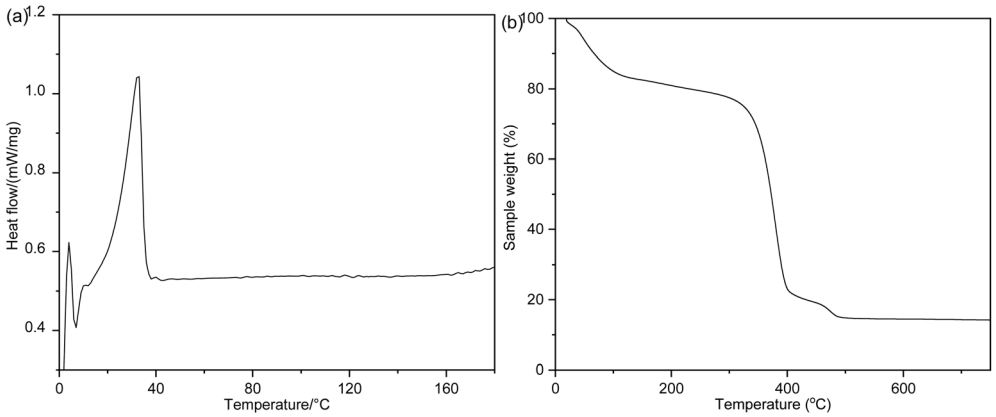

Fig. 7 The DSC thermogram (a) and TGA curve (b) of PV4A.

3.2 Performance measurements

3.2.1 Fluidity. Based on the successful synthesis of PPEGMA–PVPA, its application potential as a new cement superplasticizer has been explored.

The effects of PPEGMA–PVPA on the fluidity of cement paste were investigated and compared with the reference PPEGMA–PAA, and the time evolution of cement paste fluidity incorporated with synthesized polymers are exhibited in Fig. 8. The water/cement (w/c) ratio of the cement paste without polymers was 0.29, and the dosage of synthesized polymers was 0.15% by cement weight. As shown in Fig. 8, the dispersing capacity of PPEGMA–PVPA was closely related to the content of the phosphorous anchor group, and the initial fluidity of the cement paste incorporated with PV4A was the greatest, followed by PV3A and PV2A. The initial flow of the reference PPEGMA–PAA was close to that of PV3A. Because the cement paste incorporated with PV1A almost lost fluidity under this condition, the data of PV1A are not included in Fig. 8. In addition, the fluidity retention properties of the synthesized polymers were investigated. The fluidity of the cement paste incorporated with PPEGMA–PVPA decreased slightly with time, and the fluidity of the cement paste incorporated with PPEGMA–PAA was more significantly impaired than that with PV2A after 60 min. The above results may be attributed to the difference of the adsorption capacity of the synthesized polymers onto the cement pastes. For the comb-type superplasticizers, the anionic anchor moieties can form chelation complexes with calcium ions to promote the adsorption capacity. Thus, a higher adsorption amount of superplasticizers always results in a stronger retardation effect on the formation of hydration products, and causes changes in the water-reducing and slump retention performance.[30]

3.2.2 Adsorption performance. The adsorption capacity of the synthesized polymers onto cement were tested by means of a TOC analyzer. The percentage of synthesized polymers was equal to 0.10–0.25% with respect to the cement content (bwoc). The amounts of polymers absorbed as a function of time were recorded in Fig. 9a, and the time needed to reach equilibrium and the saturation amount were determined. The adsorption amounts of the phosphate-containing polymers and reference polycarboxylate polymer on the cement pastes increased with time, and reached the maximum value after 30 minutes at a dosage of 0.15% bwoc. The effects of the polymer dosages on adsorption performance of PV4A, PV3A, PV2A and PPEGMA–PAA were also investigated. As shown in Fig. 9b, the adsorption amounts of these polymers increased with increasing dosage, and the equilibrium values of PV4A and PV3A were higher than that of PPEGMA–PAA, despite the actual ratios of the anchor moieties in PPEGMA–PAA and PV4A being similar. The obvious difference of the adsorption behavior indicated that the adsorption capacity of the phosphate group onto the cement was indeed stronger than that of the carboxylate group.

3.2.3 Zeta potential analysis. Furthermore, the zeta potential analysis was employed to characterize the adsorption behavior of the synthesized polymers onto cement pastes. The adsorption of anion-charged polymers on the surface of the

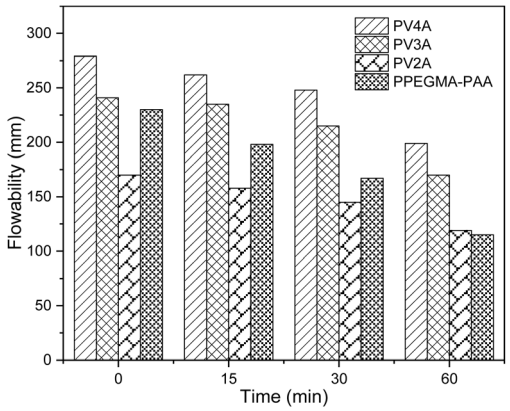

Fig. 8 Time evolution of the fluidity of cement paste incorporated with synthesized polymers.

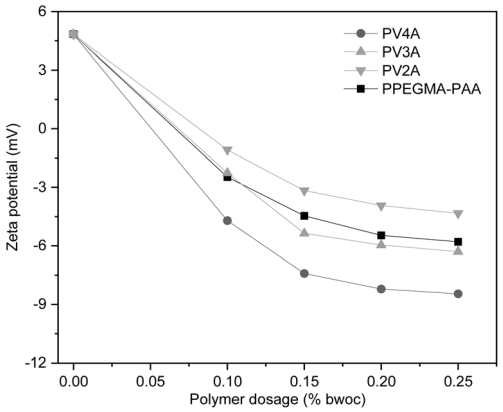

Fig. 10 Zeta potential of cement paste incorporated with synthesized polymers at various dosages.

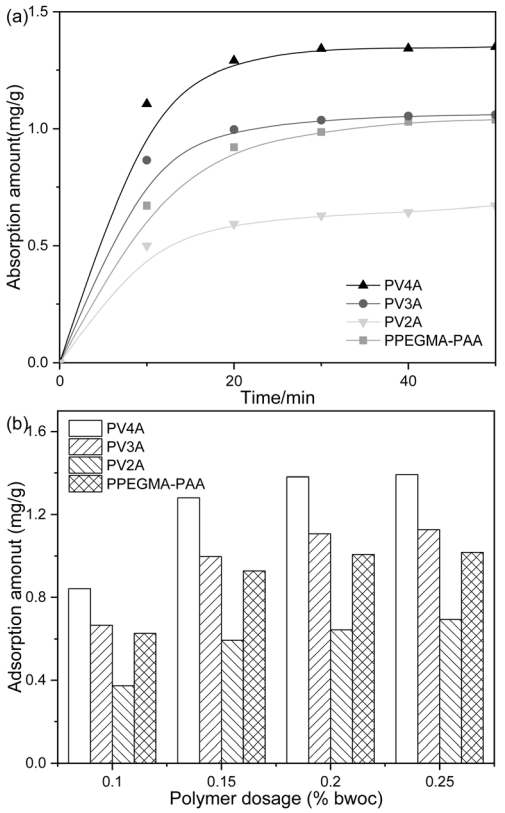

Fig. 9 The adsorption performance of PV4A, PV3A, PV2A and PPEGMA–PAA onto cement. (a) Adsorption amount over time at 0.15% bwoc dosage; (b) adsorption saturation amount against polymer dosage.

cement pastes could cause the change in the surface charge distribution and hydration layer thickness, which in turn could affect the zeta potential of the cement paste. As shown in Fig. 10, before adding the synthesized polymers, the cement paste had a positive zeta potential value (4.8 mV), which would promote the adsorption of anion-charged polymers by electrostatic adherence. The addition of the synthesized polymers caused a remarkable decrease of the zeta potential value. Furthermore, with the dosage increase, the zeta potential value of the polymers became more negative until reaching the saturation value. As mentioned in the adsorption test, the adsorption of PPEGMA–PVPA basically reached the saturation amount at a high dosage (>0.2% bwoc). Thus, the absolute zeta potential value also reached stable values. Although the molar ratio of the anionic anchor moieties to PEGMA in PV4A and PPEGMA–PAA were all close to 75%, the higher negative-charge density of the phosphate group made the absolute zeta potential value of PV4A (−7.4 mV) larger at 0.15% bwoc dosage. Furthermore, even the absolute zeta potential of PV3A (−5.3 mV) was slightly larger than that of PPEGMA–PAA (−4.4 mV). Due to the lower adsorption amount of PV2A, the zeta potential value of PV2A (−3.1 mV) was the smallest at 0.15% bwoc dosage in these synthesized polymers.

4 Conclusions

In summary, a novel superplasticizer PPEGMA–PVPA containing a phosphate group was synthesized by solution radical copolymerization using VPA and PEGMA as monomers. The actual ratios of two monomers in synthesized polymers were determined, and the ^{1}H NMR and ICP-AES analysis showed that about 70% of the feed VPA monomer was reacted in the copolymerization. The effect of the monomer proportion on the adsorption–dispersion performance was investigated and compared with a reference polycarboxylate superplasticizer. The TOC results indicated that the adsorption capacity of PPEGMA–PVPA was about 1.4 times stronger than that of the reference polycarboxylate superplasticizer. Thus, PPEGMA–PVPA demonstrated stronger dispersion and water-reducing capacity. The results suggest that PPEGMA–PVPA has satisfactory adsorption–dispersion performance and provides another option for the cement superplasticizer.

Conflicts of interest

There are no conflicts to declare.

Acknowledgements

The authors gratefully acknowledge the financial supports from the Youth Fund of the National Natural Science Foundation of China (No. 52108218).

References

1 S. Sha, M. Wang, C. Shi and Y. Xiao, *Constr. Build. Mater.*, 2020, **233**, 117257.
2 K. Karakuzu, V. Kobya, A. Mardani-Aghabaglou, B. Felekoğlu and K. Ramyar, *Constr. Build. Mater.*, 2021, **312**, 125366.
3 K. Yamada, T. Takahashi, S. Hanehara and M. Matsuhisa, *Cem. Concr. Res.*, 2000, **30**, 197–207.
4 B. Felekoğlu and H. Sarıkahya, *Constr. Build. Mater.*, 2008, **22**, 1972–1980.
5 F. R. Kong, L. S. Pan, C. M. Wang and N. Xu, *Constr. Build. Mater.*, 2016, **105**, 545–553.
6 Q. Ran, X. Wang, J. Jiang and Y. Yang, *Adv. Cem. Res.*, 2016, **28**, 202–208.
7 J. Stecher and J. Plank, *J. Colloid Interface Sci.*, 2020, **562**, 204–212.
8 J. Stecher and J. Plank, *Cem. Concr. Res.*, 2019, **119**, 36–43.
9 M. L. Vo and J. Plank, Dispersing effectiveness of a phosphated polycarboxylate in α-and β-calcium sulfate hemihydrate systems, *Constr. Build. Mater.*, 2020, **237**, 117731.
10 Y. He, X. Zhang and R. D. Hooton, *Constr. Build. Mater.*, 2017, **132**, 112–123.
11 J. Plank, F. Yang and O. Storcheva, *J. Sustainable Cem.-Based Mater.*, 2014, **3**, 77–87.
12 W. Fan, F. Stoffelbach, J. Rieger, L. Regnaud, A. Vichot, B. Bresson and N. Lequeux, *Cem. Concr. Res.*, 2012, **42**, 166–172.
13 H. Qi, B. Ma, H. Tan, Y. Su, Z. Jin, C. Li, X. Liu, Q. Yang and Z. Luo, *Constr. Build. Mater.*, 2021, **271**, 121566.
14 B. Wang, S. Qi, S. Fan, T. Wang, J. Ma, Z. Han and Q. Ran, *J. Dispersion Sci. Technol.*, 2019, **41**, 742–750.
15 N. Moszner, *Dental Praxis*, 2001, **18**, 105–112.
16 L. Macarie and G. Ilia, *Prog. Polym. Sci.*, 2010, **35**, 1078–1092.
17 Z. Taherkhani, M. Abdollahi and A. Sharif, *J. Polym. Res.*, 2017, **24**, 1–10.
18 K. H. Markiewicz, L. Seiler, I. Misztalewska, K. Winkler, S. Harrisson, A. Z. Wilczewska, M. Destarac and J. D. Marty, *Polym. Chem.*, 2016, **7**, 6391–6399.
19 R. E. Dey, X. Zhong, P. J. Youle, Q. G. Wang, I. Wimpenny, S. Downes, J. A. Hoyland, D. C. Watts, J. E. Gough and P. M. Budd, *Macromolecules*, 2016, **49**, 2656–2662.
20 I. Blidi, R. Geagea, O. Coutelier, S. Mazières, F. Violleau and M. Destarac, *Polym. Chem.*, 2012, **3**, 609–612.
21 J. Tan, R. A. Gemeinhart, M. Ma and W. M. Saltzman, *Biomaterials*, 2005, **26**, 3663–3671.
22 V. Najafi, K. Kabiri, F. Ziaee, H. Omidian, M. J. Zohuriaan-Mehr, H. Bouhendi and H. Farhadnejad, *J. Polym. Res.*, 2012, **19**, 1–7.
23 L. K. Tomar, C. Tyagi, S. S. Lahiri and H. Singh, *Polym. Adv. Technol.*, 2011, **22**, 1760–1767.
24 B. Bingöl, W. H. Meyer, M. Wagner and G. Wegner, *Macromol. Rapid Commun.*, 2006, **27**, 1719–1724.
25 L. Seiler, J. Loiseau, F. Leising, P. Boustingorry, S. Harrisson and M. Destarac, *Polym. Chem.*, 2017, **8**, 3825–3832.
26 N. Zhang, S. Salzinger and B. Rieger, *Macromolecules*, 2012, **45**, 9751–9758.
27 J. Plank, C. Schroefl, M. Gruber, M. Lesti and R. Sieber, *J. Adv. Concr. Technol.*, 2009, **7**, 5–12.
28 H. Komber, V. Steinert and B. Voit, *Macromolecules*, 2008, **41**, 2119–2125.
29 J. Deng, Y. Shi, W. Jiang, Y. Peng, L. Lu and Y. Cai, *Macromolecules*, 2008, **41**, 3007–3014.
30 Q. Ran, M. Qiao and J. Liu, *Iran. Polym. J.*, 2014, **23**, 663–669.